Experimental and theoretical studies of the molecular structure of 1-(2-pyridinylmethyl)-2-methylbenzimidazole

ARTICLE *in* JOURNAL OF MOLECULAR STRUCTURE · APRIL 2010

Impact Factor: 1.6 · DOI: 10.1016/j.molstruc.2010.01.011

2 AUTHORS, INCLUDING:

Samuel P Hernández-Rivera
University of Puerto Rico at Mayagüez
210 PUBLICATIONS **958** CITATIONS

Journal of Molecular Structure 968 (2010) 6–12

Contents lists available at ScienceDirect

Journal of Molecular Structure

journal homepage: www.elsevier.com/locate/molstruc

Experimental and theoretical studies of the molecular structure of 1-(2-pyridinylmethyl)-2-methylbenzimidazole

Ricardo Infante-Castillo [a,*], Samuel P. Hernández-Rivera [b]

[a] Department of Physics–Chemistry, University of Puerto Rico-Arecibo, P.O. Box 4010, Arecibo, PR 00613-4010, Puerto Rico
[b] Department of Chemistry, University of Puerto Rico-Mayagüez, Call Box 9000, Mayagüez, PR 00681-9000, Puerto Rico

ARTICLE INFO

Article history:
Received 22 October 2009
Received in revised form 29 December 2009
Accepted 5 January 2010
Available online 11 January 2010

Keywords:
2-Methylbenzimidazole
2-Picoline
GIAO
DFT
Chemical shifts

ABSTRACT

In this work, we report a combined experimental and theoretical study on the molecular structure and vibrational spectra of 1-(2-pyridinylmethyl)-2-methylbenzimidazole. The structure of the target compound has been proposed by elemental analysis and spectroscopic data, i.e., IR, Raman, UV, MS, ^{1}H and ^{13}C NMR. The experimental results were supported by performing DFT calculations for the ground state geometry, electronic structure and vibrational spectra using the B3LYP functional and the 6-311+G** basis set. The optimized geometric bond lengths and bond angles obtained by using DFT have been compared with X-ray diffraction values available in the literature for the precursors (2-methylbenzimidazole and 2-picoline), as a polycrystalline structure of this compound could not be obtained in this experiment. All the experimental vibrational bands have been discussed and assigned to normal mode on the basis of our calculations. Good linear correlation between the experimental ^{1}H and ^{13}C NMR chemical shifts in DMSO-d_6 solution and calculated GIAO shielding tensors were found.

1. Introduction

The benzimidazole scaffold is an accepted pharmacophore and represents an important synthetic precursor in new drug discovery [1–8]. It is also of considerable interest as a ligand towards transition metal ions in a variety of biological molecules [9,10]. At the same time, derivatives of picoline have potent hypolipidemic effects, antineoplastic and anti-inflammatory activities and show good activity against leukemia and human glioma cell growth [11]. In connection with our investigations in the field of N-substituted benzimidazoles, we extended our studies to the synthesis and characterization of potentially biological useful compounds from the reaction of 2-picolyl chloride hydrochloride with 2-methylbenzimidazole. Fig. 1 shows the numbering of the atoms in the structure of 1-(2-pyridinylmethyl)-2-methylbenzimidazole. Recently, we reported studies on the structural properties of two 1-alkyl-2-methylbenzimidazoles compounds [12], on the isomers of 1-propenyl-2-methylbenzimidazoles [13] and on the isomers of 1-(2-methylpropenyl)-2-methylbenzimidazole [14]. In the present work, 1-(2-pyridinylmethyl)-2-methylbenzimidazole was synthesized and then IR, UV, Raman and NMR spectroscopy techniques were used to validate its structure. In addition, the molecular geometry, absorption wavelengths and vibrational spectra of the title compound ($C_{14}H_{13}N_3$) were calculated by applying density functional theory computations using Becke's three-parameter hybrid functional method [15] with Lee, Yang and Parr's correlation functional [16] and the 6-311+G** basis set. The calculated geometric parameters and vibrational frequencies were analyzed theoretically and then compared with obtained experimental results. In addition, GIAO (gauge-independent atomic orbital) [17] ^{13}C and ^{1}H calculations of this derivative of 2-methylbenzimidazole have been calculated by using the B3LYP method with the 6-311+G** basis set. The solvent effects on NMR data were introduced by the Integral Equation Formulation-Polarizable Continuum Model (IEF-PCM) method [18] implemented in the GAUSSIAN 03 program [19]. These calculations were valuable for providing insight into molecular parameters, and vibrational and NMR spectra. In this article, we present basic experimental and theoretical information about the structure of a 1-(2-pyridinylmethyl)-2-methylbenzimidazole. To the best of our knowledge, no evidence of similar studies for this derivative of 2-methylbenzimidazole has been reported to date in the open chemical literature.

2. Experimental and calculations

2.1. Synthesis

All chemicals used for the preparation of the title compound were of reagent grade quality. The 1-(2-pyridinylmethyl)-2-methylbenzimidazole compound was prepared by a modified method that was used for N-alkylation of indoles and pyrroles [20]. Potassium hydroxide (KOH, 2.13 g, 37.9 mmol) was dissolved in 25.0 mL of

* Corresponding author.
E-mail addresses: ricinfante@gmail.com, ric12921@uprm.edu (R. Infante-Castillo).

0022-2860/$ - see front matter © 2010 Elsevier B.V. All rights reserved.
doi:10.1016/j.molstruc.2010.01.011

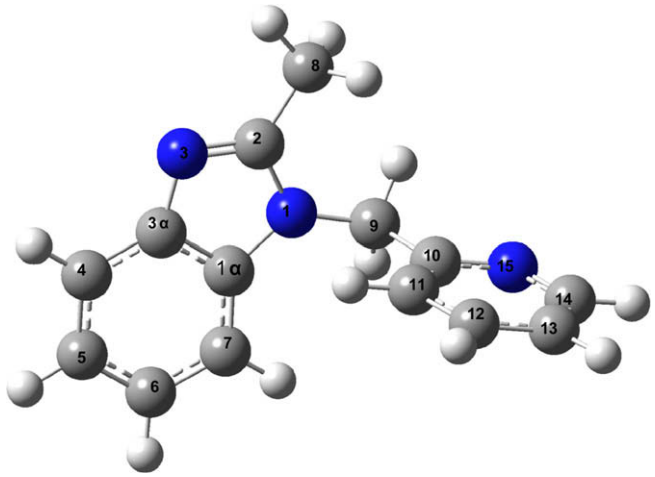

Fig. 1. Atom numberings and optimized structure of 1-(2-pyridinylmethyl)-2-methylbenzimidazole from B3LYP/6-311+G** calculations.

dimethylsulfoxide (352 mmol) with stirring in a 250 mL round-bottomed flask under a dry N_2 atmosphere. 2-Methylbenzimidazole (3.01 g, 22.8 mmol) was added and the mixture was stirred for 2 h. Upon transferring 2-picolyl chloride hydrochloride (3.80 g, 23.2 mmol), the solution turned violet after a few minutes. The reacting mixture was stirred at room temperature for 24 h under a dry N_2 atmosphere, and then products were diluted with dichloromethane and washed successively with water. The organic layer was dried over anhydrous Na_2SO_4 and the solvent was removed. The purified product was isolated and analyzed by GC–MS. The 1-(2-pyridinylmethyl)-2-methylbenzimidazole was obtained as a white solid. Yield 43%; mp 57–59 °C; mass spectrum produced by electron impact (EI) ionization showed *m/z*: 223($M^{+\cdot}$), 208, 145, 131, 118, 104, 93, 77, 65, 51, 39. Anal. Calc. for $C_{14}H_{13}N_3$: C, 75.34%; H, 5.83%; N, 18.83%. Found: C, 75.37%; H, 5.84; N, 18.81%.

2.2. Physical methods

GC–MS analyses were performed using a Hewlett Packard 5890 series II Gas Chromatograph coupled with a Hewlett Packard model 5970 mass selective detector. A Supelco SPB-5 capillary column (length: 30 m × 0.25 mm i.d.) was used for the chromatographic separation and the helium carrier gas was set to a flow rate of 0.9 mL/min. The oven temperature was initially at 70 °C (held for 10 min) and then increased to 250 °C at a rate of 10 °C/min. The mass spectrometer was operated in electron impact mode with ionization energy of 70 eV. The ion source temperature was maintained at 280 °C.

The room temperature Fourier transform infrared spectrum of the title compound was measured on a Perkin Elmer System 2000 FT-IR spectrometer in the 4000–400 cm^{-1} region with 4 cm^{-1} resolution. FT-Raman spectra were recorded on a Bruker Optics RFS-100 Fourier Transform Raman spectrometer (excitation source: Nd:YAG, 1064 nm). The measurements of the spectra were performed in the range of 100–3600 cm^{-1}, the Stokes region, with 1 cm^{-1} spectral resolution. The ^1H and ^{13}C NMR spectra were recorded on a Varian Gemini 300 FT-NMR spectrometer. The internal lock was provided by a deuterated DMSO solvent (δ = 39.51 ppm) and both proton and carbon signals were referenced to TMS. All spectra were measured at room temperature.

2.3. Computational methods

The molecular structure of the 1-(2-pyridinylmethyl)-2-methylbenzimidazole in the ground state was optimized by a DFT method with B3LYP functional and a 6-311+G** basis set. UV absorption energies and vibrational frequencies were calculated using the Configuration Interaction Singles (CIS) method [21]. The entire set of calculations was performed using the GAUSSIAN 03 W™ software (Gaussian Inc., Wallingford, CT) for Windows™ operating system (Microsoft Corp.,) and the assignment of the calculated wavenumbers was aided by the animation option of the GaussView 3.0™ graphical interface [22]. The overestimation (known systematic errors) of computed wavenumbers was compensated for by applying a wavenumber-linear scaling method (WLS) [23]. NMR calculations were performed using the GIAO method. NMR shifts were computed at the B3LYP/6-311+G** level of theory and the values for the ^1H and ^{13}C isotropic chemical shifts were referenced to the corresponding values for TMS, which was calculated at the same level of theory. The effect of solvent on the theoretical NMR parameters was included using the default IEF-PCM model provided by GAUSSIAN 03. Dimethylsulfoxide (DMSO), which has a dielectric constant (ε) of 46.7, was used as the solvent.

3. Results and discussion

3.1. Geometry optimization

The calculated molecular structure of 1-(2-pyridinylmethyl)-2-methylbenzimidazole and its numbering scheme are shown in Fig. 1. The global energy minimum obtained by DFT of the structure optimization for the title compound was −705.7897021 Hartree (-4.43×10^5 kcal mol^{-1}). The optimization studies of the picolyl derivative showed that the molecule belongs in a C_1 symmetry point group. The experimental and optimized structural parameters of 1-(2-pyridinylmethyl)-2-methylbenzimidazole calculated at the B3LYP level of theory with a 6-311+G** basis set are listed in Table 1 in accordance with the atom numbering given in Fig. 1. These values were then compared with X-ray diffraction values available in the literature for 2-methylbenzimidazole and 2-picoline [24,25]. As expected, most of the calculated C—C bond lengths for 2-methylbenzimidazole and 2-picoline were larger than the experimental values. The optimized geometry of 2-methylbenzimidazole in the ground state corresponded to C_S symmetry and the calculated bond lengths and bond angles with the computational method yielded 0.04 Å and 3° discrepancies relative to the X-ray values, respectively. For 2-picoline, the optimized geometry showed a maximum difference in bond lengths and bond angles of 0.03 Å and 0.6° between non-hydrogen atoms from the experimental values. These deviations may be attributed to the solid-state inter-molecular interactions related to the strong hydrogen bonding and crystal packing effects. Interesting, the crystal packing of 2-picoline is a $C_{(aromatic)}$—H···Π inter-molecular contact with a short H···X distance of 2.64 Å, which brought about the peculiar packing motif of 2-picoline (X is the center of the aromatic ring) [25]. Direct attachment of 2-picoline to the 2-methylbenzimidazole ring produces a small expansion in imidazole interatomic distances and all bond lengths in the pyridine ring are slightly shorter than those of the 2-picoline molecule. Significant changes, with respect to experimental and calculated values of 2-methylbenzimidazole, occur in the length of the N_1—C_2 and $C_{3\alpha}$—$C_{1\alpha}$ bonds in the imidazole ring. Also, the $C_{3\alpha}$—$C_{1\alpha}$—N_1 angle in the imidazole ring has been reduced by five degrees as a result of this substitution. In addition, it is well known that, due to low scattering factors of hydrogen atoms in X-ray diffraction, the experimental bond lengths of X—H bonds are expected to be shorter than the estimated bond lengths. The optimized C—C bond lengths in the pyridine ring fall in the range of 1.388–1.392 Å for the B3LYP/6-311+G** method, which are in good agreement with those in the crystal structure of 2-picoline (1.367–1.390 Å). The pyridine ring was found to be off-plane from

Table 1
Selected experimental and calculated geometry parameters for 2-methylbenzimidazole, 2-picoline and 1-(2-pyridinylmethyl)-2-methylbenzimidazole.

Parameters	2-Methylbenzimidazole		2-Picoline		1-(2-Pyridinylmethyl) 2-methylbenzimidazole
Bond distances (Å)	X-ray[a]	Calculated	X-ray[b]	Calculated	Calculated
N_1—C_2	1.335	1.383			1.385
C_2—N_3	1.339	1.308			1.309
N_3—$C_{3\alpha}$	1.389	1.389			1.386
$C_{3\alpha}$—$C_{1\alpha}$	1.395	1.413			1.409
$C_{1\alpha}$—N_1	1.383	1.385			1.387
$C_{3\alpha}$—C_4	1.379	1.398			1.395
C_4—C_5	1.382	1.390			1.388
C_5—C_6	1.395	1.407			1.404
C_6—C_7	1.360	1.392			1.389
C_7—$C_{1\alpha}$	1.389	1.393			1.392
C_2—C_8		1.492			1.491
N_1—C_9					1.448
C_9—C_{10}			1.498	1.507	1.520
C_{10}—C_{11}			1.390	1.399	1.392
C_{11}—C_{12}			1.376	1.391	1.390
C_{12}—C_{13}			1.367	1.391	1.388
C_{13}—C_{14}			1.379	1.393	1.391
C_{14}—N_{15}			1.337	1.334	1.332
N_{15}—C_{10}			1.332	1.342	1.337
MAD=		0.016		0.011	
RMS=		0.022		0.013	
Bond angles (°)					
N_1—C_2—N_3	112.7	112.4			112.9
C_2—N_3—$C_{3\alpha}$	106.3	105.6			105.6
N_3—$C_{3\alpha}$—$C_{1\alpha}$	107.6	110.1			110.0
$C_{3\alpha}$—$C_{1\alpha}$—N_1	107.2	110.1			105.1
$C_{1\alpha}$—N_1—C_2	106.1	107.3			106.4
$C_{3\alpha}$—C_4—C_5	118.2	118.1			118.0
C_4—C_5—C_6	121.9	121.3			121.3
C_5—C_6—C_7	120.7	121.4			121.4
C_6—C_7—$C_{1\alpha}$	117.6	116.7			116.8
C_7—$C_{1\alpha}$—$C_{3\alpha}$	122.1	122.5			122.4
C_7—$C_{1\alpha}$—N_1					132.5
$C_{1\alpha}$—N_1—C_9					126.2
N_1—C_9—C_{10}					115.6
C_9—C_{10}—C_{11}			121.6	121.8	123.2
C_9—C_{10}—N_{15}			116.6	116.3	114.1
N_{15}—C_{10}—C_{11}			121.7	121.9	122.7
C_{10}—C_{11}—C_{12}			119.4	119.3	118.6
C_{11}—C_{12}—C_{13}			118.9	118.8	119.1
C_{12}—C_{13}—C_{14}			118.5	117.9	118.1
C_{13}—C_{14}—N_{15}			123.3	123.8	123.4
MAD=		0.83		1.32	
RMS=		1.11		1.83	

MAD, mean absolute deviations; RMS, root-mean-square errors; for numbering of atoms refer to Fig. 1.
[a] Ref. [24].
[b] Ref. [25].

the benzimidazole skeleton. The value of the dihedral angles C_2—N_1—C_9—C_{10} and C_2—N_1—C_9—C_{11} was found to be 92 and 86°, respectively. The DFT predicted N_1—C_9 and C_9—C_{10} bond distances of 1.448 and 1.520 Å correspond to the bonds between the pyridine ring and the 2-methylbenzimidazole ring. All the bond lengths and angles were in good agreement with the experimental values, as demonstrated by the mean absolute deviations (MAD) and root-mean-square errors (RMS). The B3LYP values for 2-methylbenzimidazole differ from experimental by 0.016 Å, with an RMS error of 0.022 Å on average for the bond lengths set. Additionally, the values found for the MAD and RMS of 2-picoline were 0.011 and 0.013 Å, respectively. The MAD value for bond angles was 0.83° with an RMS error of 1.11° for 2-methylbenzimidazole. The corresponding values for 2-picoline were: 1.32 (MAD) and 1.83° (RMS).

3.2. Theoretical and experimental spectroscopic data

The calculated absorption wavelengths for benzimidazole and its N-substituted derivatives at the CIS-B3LYP level of theory are listed in Table 2, along with the corresponding experimental values. A linear relationship (R^2 = 0.96) was found between the transition energies observed experimentally, derived from the λ values for 1-(2-pyridinylmethyl)-2-methylbenzimidazole and the CIS-DFT calculated values. Substitution of hydrogen in benzimidazole by the picolyl group resulted in an experimentally observed bathochromic (red) shift of $\pi \rightarrow \pi^*$ transitions by approximately 4 nm. This trend was reproduced by the calculations, although the calculated changes are higher than the observed ones. These red shifts indicated conjugation between the substituent and the imidazole ring, which raises the HOMO-energy, and thus reduces the $\pi \rightarrow \pi^*$ energy differences. The spectrum of the picolyl derivative was similar to that of the benzimidazole ring. The bands of the picolyl derivative however, were less intense and had less distinct fine structure than that of the benzimidazole parent compound.

The 1-(2-pyridinylmethyl)-2-methylbenzimidazole molecule has 30 atoms with 84 normal modes of vibration. The assignments of vibrational frequencies of this derivative based on normal mode analysis are presented in Table 3, which lists the experimental and the calculated scaled frequencies. The observed and calculated FT-IR and FT-Raman for 1-(2-pyridinylmethyl)-2-methylbenzimi-

Table 2
Observed and calculated absorption energies of benzimidazole and derivatives.

Compound	Observed λ_{max} (nm)	Calculated[a] λ_{max} (nm)
Benzimidazole	278, 272, 267, 248	250, 224, 204, 198
2-Methylbenzimidazole	280, 274, 245	251, 238, 202
1-Propenyl-2-methylbenzimidazole	283, 276, 252, 230[b]	
E-Propenyl-2-methylbenzimidazole		269, 256, 240, 231
Z-Propenyl-2-methylbenzimidazole		261, 254, 242, 230
2-Propenyl-2-methylbenzimidazole		256, 254, 244, 231
1-(2-Methylpropenyl-2-methylbenzimidazole	283, 276, 253, 228[c]	
1-(2-Methyl-1-propenyl-2-methylbenzimidazole		256, 250, 244, 233
1-(2-Methyl-2-propenyl-2-methylbenzimidazole		256, 244, 242, 230
1-(2-Pyridinylmethyl)-2-methylbenzimidazole	283, 276, 267, 254, 227	284, 261, 252, 242, 223

[a] Calculated with CIS/B3LYP 6-311+G**.
[b] Ref. [13].
[c] Ref. [14].

dazole are presented in a common frequency scale in Figs. 2 and 3, respectively. The mode number assignments were made from comparisons of experimental spectra and the theoretical calculations. Very weak signals were not labeled. It is important to mention that the theoretical results refer to the isolated molecule in the gas phase, whereas comparisons were made with FT-IR and FT-Raman spectra of the solid sample. In general, the IR gas-phase spectra were found to be advantageous over the solution or solid phase spectra because the symmetry of most vibrational coordinates is easily determined from the rotational profiles of the IR bands, and hydrogen bond formation and other inter-molecular interactions are mostly avoided. Some of the differences in the calculated spectra were evident in the intensities of the bands. The overestimation of computed wavenumbers was corrected using a wavenumber-linear scaling method (WLS) with the following relationship:

Table 3
Observed and calculated selected frequencies (cm^{-1}) and assignments of the fundamental modes for 1-(2-pyridinylmethyl)-2-methylbenzimidazole.

Mode No.	1-(2-Pyridinylmethyl)-2-methylbenzimidazole			
	FT-IR (cm^{-1})	FT-Raman (cm^{-1})	Calc.[a] (cm^{-1})	Assignment[b,c]
1	–	3066	3061	$\nu^{s}CH_{(Pic)}$
2	3040	–	3051	$\nu^{as}CH_{(Bz)}$, $\nu^{as}CH_{(Pic)}$
3	2964	2989	2945	$\nu^{as}CH_{(Met)}$
4	–	2920	2906	$\nu^{as}CH_2$
5	1615	1678	1620	$\nu C{=}C_{(Bz)}$
6	1592	1591	1598	$\nu C{=}C_{(Pic)}$
7	1522	1521	1534	$\nu C{=}N_{(Im)}$
8	1460	1452	1457	$\beta CH_{(Met)}$, βCH_2, $\beta CH_{(Bz)}$
9	1399	–	1399	$\gamma CH_{(Met)}$
10	–	1385	1380	$\gamma CH_{(Met)}$, γCH_2, $\beta CH_{(Bz)}$
11	1325	–	1332	$\beta CH_{(Bz)}$
12	–	1286	1293	$\beta CH_{(Bz)}$
13	1265	–	1254	$\beta CH_{(Bz)}$, γCH_2
14	–	1236	1235	γCH_2, $def_{(Im)}$
15	1152	1147	1157	$\beta CH_{(Bz)}$
16	1091	1060	1060	$\beta CH_{(Pic)}$
17	–	1010	1011	$\gamma CH_{(Met)}$, $\beta CH_{(Bz)}$
18	852	856	865	γCH_2
19	–	775	776	$rg_{\ breathing}$
20	741	–	747	$\gamma CH_{(Bz)}$
21	667	673	678	$\beta def_{(Bz+Im)}$
22	624	–	629	$\beta def_{(Pic)}$
23	579	–	519	$\gamma CH_{(Bz)}$
24	–	500	500	$\beta def_{(Bz+Im)}$

[a] Calculated with B3LYP/6-311+G**; scaled, according to correlation equation $\nu_{obs}/\nu_{calc} = 1.0087(9) - 0.0000163(6)\ (\nu_{calc}/cm^{-1})$ [22].
[b] *Vibrational modes:* ν, stretching; β, in-plane bending; γ, out-of plane bending; rg, ring; def, deformation; superscript s, symmetric; superscript as, anti-symmetric; Bz, benzene; Pic, 2-picoline; Im, imidazole; Met, methyl.
[c] Estimated graphical representation.

$$\nu_{obs}/\nu_{calc} = 1.0087(9) - 0.0000163(6)(\nu_{calc}/cm^{-1}) \quad (1)$$

A strong FT-Raman absorption at 3066 cm^{-1} [1] was assigned to the CH symmetric stretching mode, ν_{C-H}, of the pyridine ring. The two weak FT-IR bands [2,3] observed in the region 2900–3200 (not shown in Fig. 2) were readily assigned to the ν_{C-H} anti-symmetric stretching modes associated with the benzene/picoline ring and alkyl group, respectively. The C—H stretching vibrations of the methyl [3] and methylene groups [4] in the FT-Raman spectrum were observed at 2989 and 2920 cm^{-1}, respectively. The deviations of these modes can be related to the crystal packing and/or the molecular aggregation that takes place when the rings of benzimidazole and 2-picoline are coupled. DFT methods, however, are known to overestimate the C—H stretching frequencies. The C=C stretching (aromatic) vibrations have characteristics bands in both experimental FT-IR and FT-Raman spectra, covering the region from 1500 to 1680 cm^{-1} [5,6]. Mode number 5 is attributed to the benzene ring and mode number 6 corresponds to the pyridine ring. In the present work, the $\nu_{C=N}$ [7] mode was found at 1522 and 1521 cm^{-1}, while the C—H in-plane modes (β_{C-H}) of benzene gave rise to a series of bands (modes 11, 12, 13 and 15) in the spectral range 1050–1325 cm^{-1}, as shown in Table 3. Similarly, the β_{C-H} of the pyridine ring was observed at 1091 cm^{-1} and the C—H out-of-plane bending mode (γ_{C-H}) of the methyl groups was found at 1399 and 1385 cm^{-1} [9,10].

Mode 10 showed considerable mixing with the in-plane bending motions of the ring. The bands obtained at 1236 and 856 cm^{-1} [14,18] are assigned to the methylene out-of-plane bending mode (γCH_2), while the CH ring out-of-plane modes appeared as two bands at 741 and 579 cm^{-1} [20,23]. The ring-breathing mode [19] in the FT-Raman spectrum located, at 775 cm^{-1}, was in agreement with the theoretical computed value. The remaining modes [21,22,24] in the 700–500 cm^{-1} region were associated with the deformations of the benzene, pyridine and imidazole rings. These corresponded to a mix of vibration modes, such as ring breathing, C—H out-of-plane modes (γ_{C-H}) and ring skeletal in-plane and out-of-plane deformations (β_{C-C-C} and γ_{C-C-C}). As can be observed from Table 3, there are some discrepancies in the agreement between calculated and experimental frequencies that could be accounted for by the probable existence of the molecule as a dimer in its solid state. However, the overall assignments are in agreement with typical values recently reported for the benzimidazole ring [26,27] and for 2-picoline [28].

3.3. ^{1}H and ^{13}C NMR spectra

In order to provide an unambiguous assignment of ^{13}C and ^{1}H NMR spectra of the studied compound, we undertook a series of NMR calculations using GIAO approximation, and results of these

calculations are shown in Table 4. The ^{1}H and ^{13}C shieldings were converted into the predicted chemical shifts using δTMS values, calculated at the same level of theory ($\delta C = 191.77$ ppm and $\delta H = 31.76$ ppm). The calculations reported here were performed in solution with DMSO as solvent using an IEF-PCM model, rather than in the gas phase. These calculations are directly comparable with experimental chemical shifts obtained in DMSO solutions. Results of linear regression fits between experimental and calculated

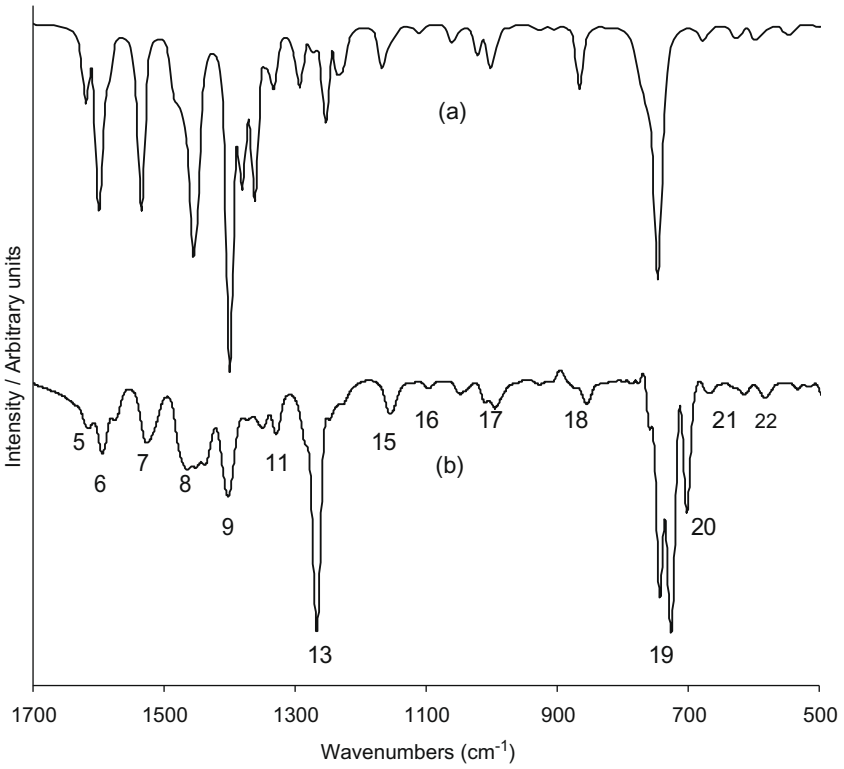

Fig. 2. Theoretical and experimental FT-IR spectra from 500 to 1700 cm^{-1} for 1-(2-pyridinylmethyl)-2-methylbenzimidazole: (a) calculated and (b) observed.

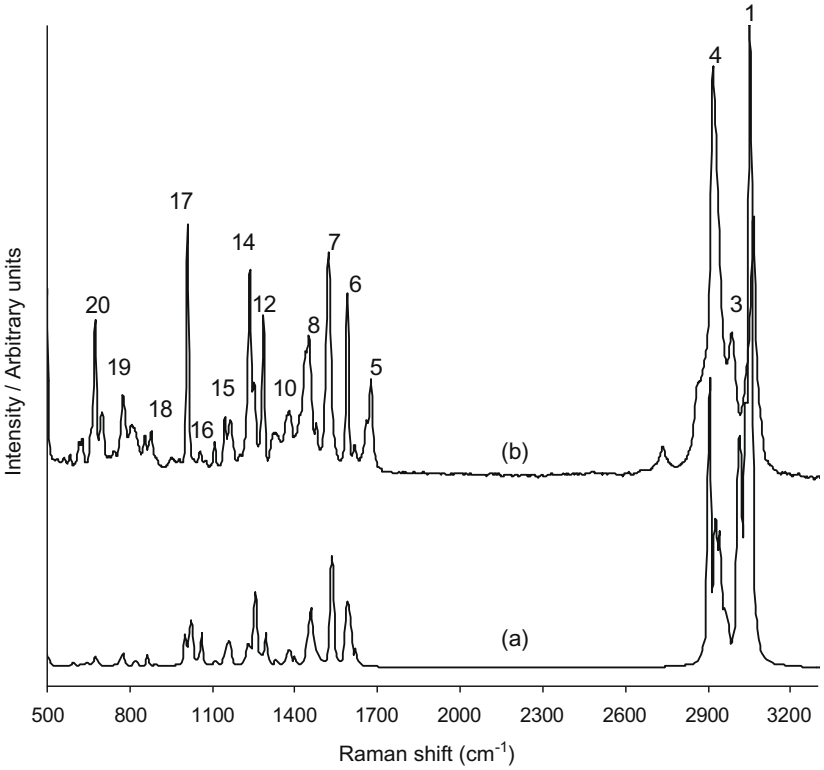

Fig. 3. Theoretical and experimental FT-Raman spectra from 450 to 3200 cm^{-1} for 1-(2-pyridinylmethyl)-2-methylbenzimidazole: (a) calculated and (b) observed.

Table 4
The experimental and theoretical ^{1}H and ^{13}C NMR chemical shifts δ(ppm) from TMS for 1-(2-pyridinylmethyl)-2-methylbenzimidazole.

Atom	^{13}C NMR		Atom	^{1}H NMR	
	δ(exp.)	δ(calc.)		δ(exp.)	δ(calc.)
$C_{1\alpha}$	135	141	H_4	7.8	8.1
C_2	152	159	$H_{5,6}$	7.3	7.7
$C_{3\alpha}$	149	150	H_7	7.3	7.7
C_4	118	123	H_8	2.6	2.5
C_5	121	126	H_9	5.5	5.6
C_6	121	126	H_{11}	7.1	6.5
C_7	109	112	H_{12}	7.5	8.0
C_8	14	14	H_{13}	7.3	7.7
C_9	48	52	H_{14}	8.5	9.1
C_{10}	155	164			
C_{11}	121	122			
C_{12}	137	143			
C_{13}	122	126			
C_{14}	149	156			
a	0.964			0.963	
R^2	0.998			0.986	
MAE	4			0.4	
RMS	5			0.4	

a, slope; R^2, correlation coefficient; MAE, mean absolute error; RMS, root-mean-square error.

chemical shifts (^{1}H and ^{13}C) performed for the structures tested are also included in Table 4. The correlation between predicted and observed carbon chemical shifts of the title compound is shown in Fig. 4. The theoretical results were in remarkably good agreement with the experimental values, with mean absolute error (MAE) no greater than 4 ppm and 0.4 ppm for ^{13}C NMR and ^{1}H NMR, respectively. The regression coefficients between the calculated and experimental chemical shifts were 0.986 for ^{1}H NMR and 0.998 for ^{13}C NMR data. The high linear correlation coefficients (R^2) and low MAE values established the robustness of the assignments. The carbon NMR spectrum showed only 12 peaks with different intensities (10 in the aromatic region), while 14 were present in the molecular formula. This suggests the presence of symmetry, which makes some of the carbon atoms equivalent. We found that the peak at 14 ppm corresponds to the methyl carbon (atom 8 in Fig. 1). Substitution of a hydrogen atom by a 2-picolyl group causes small downfield shifts of the signals assigned to carbons in the imidazole ring. The peak at 48 ppm is a deshielded (C_9) carbon situated between the benzimidazole and pyridine rings. Except for methyl protons (2.5 ppm), all the experimental chemical shifts were found to be smaller than the calculated values. The largest deviations from the experimental values were observed in the low field region of the spectra. As can be seen from the analysis of the data in Table 4, the results of GIAO/DFT calculations were found to be in excellent agreement with experimental values.

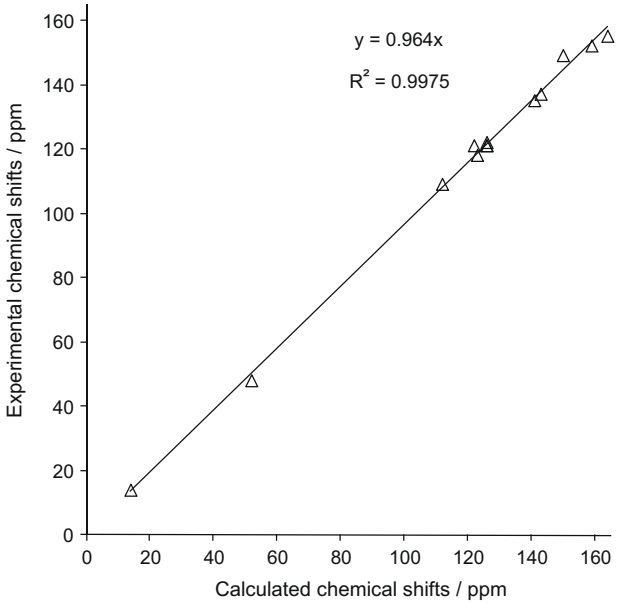

Fig. 4. The linear regression between experimental and theoretical DFT predicted ^{13}C NMR chemical shifts for 1-(2-pyridinylmethyl)-2-methylbenzimidazole, using the 6-311+G** basis set.

4. Conclusions

In an effort to prepare a new compound with potential biological activity, we have synthesized and characterized 1-(2-pyridinylmethyl)-2-methylbenzimidazole by elemental analysis, ^{1}H, ^{13}C NMR, UV, FT-IR and FT-Raman spectroscopy. The vibrational bands observed in FT infrared and FT-Raman spectra of this compound were assigned and supported by theoretically calculated (scaled) DFT vibrational spectra. GIAO NMR calculations provided chemical shift values that were in excellent agreement with experimental data. These data have been used for unambiguous assignment of the experimental ^{1}H and ^{13}C NMR signals.

Acknowledgments

We thank the Chemical Imaging Center and the Center for Chemical Sensors Development of the Department of Chemistry of the University of Puerto Rico-Mayagüez for their financial support of this project.

References

[1] J. Cheng, X. Jiangtao, L. Xianjin, Bioorg. Med. Chem. Lett. 17 (2005) 267.
[2] Y. He, J. Yang, W. Baogen, L. Risen, E. Swayze, Bioorg. Med. Chem. Lett. 14 (2004) 1217.
[3] M.A. Ismail, R. Brun, T. Wenzler, F.A. Tanious, D. Wilson, D.W. Boykin, Bioorg. Med. Chem. 12 (2004) 5405.
[4] H. Nakano, T. Inoue, N. Kawasaki, H. Miyataka, H. Matsumoto, T. Taguchi, N. Inagaki, Bioorg. Med. Chem. 8 (2000) 373.
[5] R. Marquis, J. Sheng, T. Nguyen, J. Baldeck, J. Olsson, Arch. Oral. Biol. 51 (2006) 1015.
[6] A. Ts. Mavrova, K. Anichina, D. Vuchev, J. Tsenov, P. Denkova, M. Kondeva, M. Micheva, Eur. J. Med. Chem. 41 (2006) 1412.
[7] S.O. Podunavac-Kuzmonovic, L.M. Leovac, N.V. Perisicjanjic, J. Rogan, J. Balaz, J. Serb, Chem. Soc. 64 (1999) 381.
[8] M. Boiani, M. Gonzalez, Mini Rev. Med. Chem. 5 (2005) 409.
[9] A. Khalafi-Nezhad, S. Rad, H. Mohabatkar, Z. Asraria, Bioorg. Med. Chem. 13 (2005) 1931.
[10] L.S. Ahuja, I. Prasad, Inorg. Nucl. Chem. Lett. 12 (1976) 777.
[11] M.K. Das, P.K. Maiti, S. Roy, M. Mittakanli, K.W. Morse, I.H. Hall, Arch. Pharm. Weinheim 325 (1992) 267.
[12] R. Infante-Castillo, L. Rivera-Montalvo, S.P. Hernandez-Rivera, J. Mol. Struct. 877 (2007) 10.
[13] R. Infante-Castillo, S.P. Hernandez-Rivera, J. Mol. Struct. 892 (2008) 477.
[14] R. Infante-Castillo, S.P. Hernandez-Rivera, J. Mol. Struct. 917 (2009) 158.
[15] A.D. Becke, J. Chem. Phys. 98 (1993) 5648.
[16] C. Lee, W. Yang, R.G. Parr, Phys. Rev. B37 (1988) 785.
[17] R. Ditchfield, Chem. Phys. 76 (1972) 5688.
[18] B. Menucci, J. Tomasi, J. Chem. Phys. 106 (1997) 5151.
[19] M.J. Frisch, G.W. Trucks, H.B. Schlegel, G.E. Scuseria, M.A. Robb, J.R. Cheeseman, V.G. Zakrzewski, J.A. Montgomery Jr., R.E. Stratmann, J.C. Burant, S. Dapprich, J.M. Millam, A.D. Daniels, K.N. Kudin, M.C. Strain, O. Farkas, J. Tomasi, V. Barone, M. Cossi, R. Cammi, B. Mennucci, C. Pomelli, C. Adamo, S. Clifford, J. Ochterski, G.A. Petersson, P.Y. Ayala, Q. Cui, K. Morokuma, D.K. Malick, A.D. Rabuck, K. Raghavachari, J.B. Foresman, J. Cioslowski, J.V. Ortiz, A.G. Baboul, B.B. Stefanov, G. Liu, A. Liashenko, P. Piskorz, I. Komaromi, R. Gomperts, R.L. Martin, D.J. Fox, T. Keith, M.A. Al-Laham, C.Y. Peng, A. Nanayakkara, C. Gonzalez, M. Challacombe, P.M.W. Gill, B.G. Johnson, W. Chen, M.W. Wong, J.L. Andres, M. Head-Gordon, E.S. Replogle, J.A. Pople, GAUSSIAN 03 (Revision A.9), Gaussian, Inc., Pittsburgh, 2003.
[20] O. Cox, L. Rivera, M. Cadiz, Inorg. Chim. Acta 151 (1992) 209.
[21] J.B. Foresman, M. Head-Gordon, J.A. Pople, M.J. Frisch, J. Phys. Chem. 96 (1992) 135.
[22] GaussView Computer Program Ver. 3.0, Gaussian Inc., Pittsburgh, PA, USA, 2003.

[23] H. Yoshida, K. Takeda, J. Okamura, A. Ehara, H. Matsuura, J. Phys. Chem. A 106 (2002) 3580.
[24] A.E. Obodovskaya, Z.A. Starikova, S.N. Belous, I.E. Pokrovskaya, J. Struct. Chem. 32 (1991) 421.
[25] I.I. Vorontsov, L. Almásy, M.Yu. Antipin, J. Mol. Struct. 610 (2002) 271.
[26] M.A. Morsy, A. Al-Khadi, A. Suwaiyan, J. Phys. Chem. A 106 (2002) 9196.
[27] V. Krishnakumar, S. Seshadri, S. Muthunatasen, Spectrochim. Acta Part A 68 (2007) 811.
[28] J.F. Arenas, I. Lopez, J.C. Otero, J.I. Marcos, J. Mol. Struct. 410–411 (1997) 443.